Physics Letters A 378 (2014) 2423–2428

Contents lists available at ScienceDirect

Physics Letters A

www.elsevier.com/locate/pla

The effect of an external signal on output microwave power of a low-voltage vircator

N.S. Phrolov [a,b], A.A. Koronovskii [a,b], Yu.A. Kalinin [a], S.A. Kurkin [a,b], A.V. Starodubov [a,b], A.E. Hramov [a,b,*]

[a] Saratov State Technical University, Politehnicheskaja 77, Saratov 410028, Russia
[b] Saratov State University, Astrahanskaja 83, Saratov 410012, Russia

ARTICLE INFO

Article history:
Received 4 March 2014
Received in revised form 16 June 2014
Accepted 21 June 2014
Available online 25 June 2014
Communicated by F. Porcelli

Keywords:
Vircator
Overcritical electron beam
Virtual cathode
Output power gain
Nonlinear dynamics
External signal
Microwave radiation

ABSTRACT

This Letter is devoted to results of the both experimental and theoretical studies of electromagnetic radiation output power gain in the low-voltage microwave generator with a virtual cathode (vircator) under an external harmonic signal leading to the preliminary velocity modulation of the electron beam. The simple theoretical model of the electron beam with virtual cathode in a diode gap with retarding field under the external signal has been developed. The theoretical and numerical analysis have shown the possibility of power amplification in the vircator under the external influence. Obtained results of the theoretical consideration are proven by the experimental study.

1. Introduction

The analysis of microwave oscillations in a GHz/THz range in spatially extended systems with overcritical electron beams in regimes of a virtual cathode (VC) formation attracts the great attention of a scientific community [1–11]. Microwave generators using electron beams with a VC (the so-called *vircators*) [1,12] are perspective devices of the high-power microwave electronics for the generation of impulses of wideband microwave radiation due to its high output microwave power, a simple construction (including the possibility of operation without a focusing magnetic field), a simple frequency tuning and regime switching by varying control parameters or by different types of action on VC oscillations (e.g., external signal influence or the introduction of additional feedback) [3,5,13–20]. All these circumstances increase the fundamental and applied importance of studies of the nonlinear dynamics of electron beams with a VC.

One of the actively investigated modification of vircators is a low-voltage system based on intense non-relativistic or low-relativistic electron beams [4,21,22]. It is considered as the promising controllable source of wideband microwave radiation [4,23]. In a low-voltage vircator a non-stationary oscillating VC in an electron beam is formed in the presence of a retarding electric field. The simplest model of a low-voltage vircator is a plane diode gap consisting of two grids and pierced by an electron beam. A retarding voltage is applied to the second (output) grid of the diode region and forms the static electric field decelerating electrons that leads to the formation of a VC at lower beam currents. The variations of the retarding voltage lead to the change of power and bandwidth of the output microwave signal [4,7,24].

Several early theoretical and experimental studies were concentrated on the analysis of the effect of external signals on generation in a vircator but they were mainly related to the external and mutual synchronization of VC oscillations [3,5,25–28]. The problem of the effect of a weak external signal on microwave output power of a vircator and the possibility to create the amplifier of microwave signals based on an electron beam with a VC have yet to be investigated (practically, the sole exception is Ref. [29]).

This Letter presents results of the both theoretical analysis and experimental study of output power amplification in the non-autonomous low-voltage vircator under the external single-frequency signal influence leading to the velocity pre-modulation of the injected electron beam.

* Corresponding author.
E-mail address: hramovae@gmail.com (A.E. Hramov).

http://dx.doi.org/10.1016/j.physleta.2014.06.031
0375-9601/

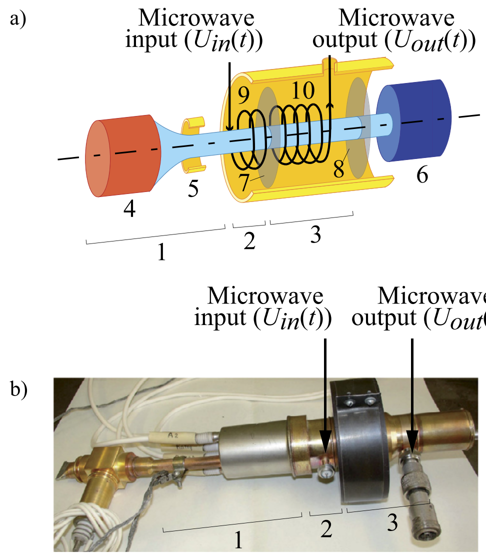

Fig. 1. Scheme (a) and external view (b) of the low-voltage vircator under study. Details of the vircator scheme: 1 – electron gun; 2 – modulation section (modulator); 3 – interaction space; 4 – cathode; 5 – anode; 6 – collector; 7 – input grid; 8 – output grid; 9 – input (modulating) helix electrodynamic system; 10 – output helix electrodynamic system.

2. Experimental setup

The experimental setup of the system under study (the low-voltage vircator) is shown in Fig. 1. We have considered the experimental model of the vircator which consists of the electron source *1*, the section *2* for the electron beam pre-modulation and the interaction space *3* with a retarding potential where the VC forms in the electron beam. The electron beam is formed by the electron gun and injected into the diode gap with a retarding field composed of two grid electrodes. The retarding field is created by means of the potential difference between grids of the diode. A thermionic cathode is used as an electron source. The electron gun with the anode (to which an accelerating voltage, V_0, is applied) forms an axially symmetric convergent cylindrical solid electron beam. The electron beam is considered as monoenergetic due to the negligible spread of electron velocities at the output plane of the electron gun region. The beam accelerating voltage is $V_0 = 1.7$ kV; the beam current $I_0 = 120$ mA; the beam radius $r_b = 5$ mm; the radius of the beam channel $R = 7.5$ mm. The external uniform magnetic field with induction $B_0 = 200$ G is applied along the longitudinal axis of the device, therefore the motion of electrons can be considered as close to one-dimensional.

Initially, the electron beam enters the area of the modulating helix system (the so-called *modulator*). In this space *2* (see Fig. 1) the electron beam is affected by an external signal. The effect of the external harmonic electric field leads to the velocity pre-modulation of the beam. Then the modulated electron beam emerges in the interaction space *3* of the low-voltage vircator.

The potential of the input grid electrode V_0 is equal to the potential of the anode, and the potential of the output grid $V_b = V_0 - \Delta V$ varies from the value $V_b/V_0 = 1$ ($\Delta V = 0$, without braking) to $V_b/V_0 = 0$ ($\Delta V = V_0$, the retarding voltage is equal to the accelerating one). Under the influence of the retarding field a non-stationary VC is formed in the electron beam of the low-voltage vircator [4]; the form and power of its oscillations depend essentially on the value of the retarding potential, V_0 [4,24,7]. VC oscillations were analyzed with the help of a helix broadband output system loaded onto an absorptive insert on the one end and onto the microwave power output on the other.

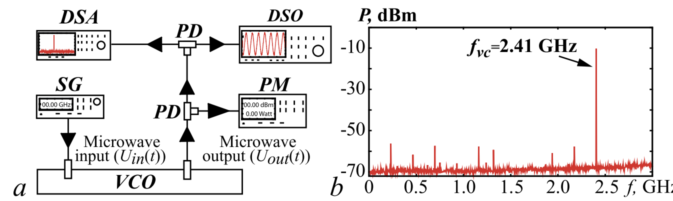

Fig. 2. (a) The block diagram of the experimental scheme for the investigation of a power amplification in the non-autonomous low-voltage vircator under the external single-frequency signal. Acronyms are: virtual cathode oscillator (VCO); power divider (PD); digital storage oscilloscope (DSO); digital spectrum analyzer (DSA); power meter (PM); signal generator (SG); (b) experimentally obtained power spectrum of the low-voltage vircator in an autonomous regime for $\Delta V = 600$ V corresponding to the periodic oscillations in the system.

The experimental vacuum setup operates with the residual gas pressure of 10^{-7} Torr. Its external view is shown in Fig. 1(b). Output microwave signals of the investigated generator are analyzed by the digital storage oscilloscope, the digital signal analyzer and the power meter and stored in a computer.[1] The block diagram of the experimental scheme is shown in Fig. 2. The low-voltage vircator generates a microwave signal with the base frequency $f_{VC} = 2.41$ GHz and output power $P_0 = 2.8$ W in an autonomous regime (see Fig. 2(b)).

3. Theoretical investigation

We have considered a 1D model of the low-voltage vircator (a 1D diode region with a retarding field pierced by an electron beam) as the object of the theoretical study. An oscillating VC in the electron beam is formed in the space of the diode region when the beam current and the retarding potential exceed some critical values [1,5]. We assume that the external harmonic signal effects through the section of the helix electrodynamic system (HES) installed between the electron source and the diode gap (interaction space) where a VC is formed. An external signal leads to the preliminary modulation of the velocity of the beam into the vircator.

The proposed simple theoretical model of an electron beam with a VC in the retarding field and under the influence of the external force is based on following assumptions. We consider the interaction drift space of the low-voltage vircator system. It is known that a VC as a potential barrier to a beam reflects partially the electron beam back to the area of injection and modulates its density and velocity at the natural frequency f_{VC}. So, the investigation of beam dynamics in such vircator system may be considered as the problem of the motion of a charged particle beam in a retarding field of a low-voltage vircator which is the sum of constant and variable components. The constant retarding field V_d is the result of the potential difference between grids of the diode gap, ΔV, and the constant potential barrier of the VC. The variable field $\tilde{V}(t) = V_{VC}e^{j\omega_{VC}t}$ ($j = \sqrt{-1}$) is the braking field of the unsteady VC that occurs due to the variable potential in the VC region. The effect of the external signal on dynamics of the electron flow is considered as the velocity modulation of the beam at the entrance of the diode region with the external force frequency $\omega_m = 2\pi f_m$.

The solution of this problem is reduced to the analysis of equations of electrons motion in the interaction space. To analyze dynamics of the electron beam in the retarding field in a VC formation regime we use dimensionless variables of longitudinal coordinate $x/x' = L$, time $t/t' = L/v_0$, frequency $f/f' = v_0/L$, and potential $V/V' = v_0^2/\eta$. Here L is the length of the interaction space (diode gap with a retarding field), v_0 is the velocity of electron beam at the anode, η is the specific electronic charge. Further we will omit the primes on the dimensionless variables.

[1] We have used the measuring equipment of Agilent Technologies company.

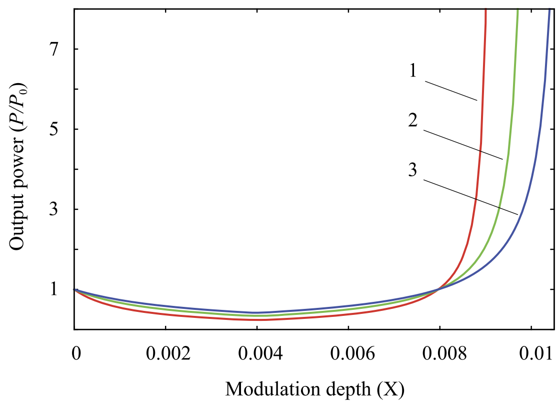

Fig. 3. Results of theoretical analysis. Analytically calculated values of output power of the low-voltage vircator under different values of a retarding potential defined by the parameter β: *1* – $\beta = 0.00517$, *2* – 0.00597, *3* – 0.00677. Parameter $\mu = 0.0039$.

According to Newton's second law dynamics of charged particles in the diode gap is described by the following equation:

$$\ddot{x} = \left(V_{VC}e^{j\omega_{VC}t} - V_d\right). \tag{1}$$

Here V_{VC} and ω_{VC} are the amplitude and the frequency of VC oscillations (the variable part of the retarding potential of the drift space), and V_d is the fixed part of the retarding potential.

Integrating (1) two times with boundary and initial conditions

$$t = t_1, \qquad x = 0, \qquad \dot{x}(0, t_1) = v_0\left(1 + X\sin(\omega_m t_1)\right) \tag{2}$$

(X is the dimensionless depth of the beam velocity pre-modulation) we obtain expressions for the coordinate, x, and the transit angle, $\phi = \omega_{VC}t$, of electrons in the diode region:

$$x = \left(1 + X\sin(\omega_m t_1)\right)(t - t_1) - \frac{V_d}{2}(t - t_1)^2 - \frac{V_{VC}}{\omega_{VC}^2}\left[e^{j\omega_{VC}t} - e^{j\omega_{VC}t_1} - j\omega_{VC}e^{j\omega_{VC}t_1}(t - t_1)\right] \tag{3}$$

$$\phi\left(1 + X\sin(\omega_m t_1)\right) = \mu\left[e^{j\phi} - j\phi - 1\right]e^{j\omega_{VC}t_1} + \beta\phi^2, \tag{4}$$

where $\mu = V_{VC}/\omega_{VC}$ is the dimensionless depth of the modulation of the electron beam in the diode region by VC oscillations and $\beta = V_d/2\omega_{VC}$ defines the effect of constant retarding field V_d.

Taking into account the charge conservation law $I(x,t)|dt| = I_0 dt_1$ we determine the bunched beam current:

$$I(x,t) = I_0\left(1 + \frac{1}{\omega_{VC}}\frac{d\phi}{dt_1}\right)^{-1}, \tag{5}$$

where I_0 is the beam current injected to the interaction space and t_1 is the time when electrons enter the interaction space. Microwave power of the low-voltage vircator is registered with the help of the output HES therefore output microwave power is proportional to the value of a bunched beam current and can be estimated as $P = \rho I^2$, where ρ is a coupling coefficient of a beam and electromagnetic wave in a HES (a coupling impedance).

The analysis of the stationary theoretical model of the electron beam with a VC in the low-voltage vircator shows the growth of output microwave power with the increase of the beam velocity pre-modulation depth at the entrance of the interaction space. Fig. 3 demonstrates the analytically obtained dependencies of normalized vircator output power P/P_0 for different amplitudes of the retarding electric field. Here P_0 is output power of the autonomous generator. One can see that the increase of the electron current velocity pre-modulation depth which is proportional to the external harmonic signal amplitude leads to the rise of output radiation power of the low-voltage vircator. According to the developed theoretical analysis of the electron beam with a stationary VC the amplification of microwave radiation power reaches $P/P_0 = 5$–10 in the range of experimentally implemented values of the modulating field. The explanation of the output power increase as a growth of the bunched beam current, $I(x,t)$, in the framework of the suggested model consists in an electron bunching improvement in the VC area due to the beam velocity pre-modulation by the external signal. In the absence of the external signal the electron beam is bunched in the only modulating field of the oscillating VC which is relatively weak. The presence of the additional pre-modulation leads to the significant improvement of a bunching in the VC area. Fig. 3 also demonstrates the insignificant decline of value P/P_0 at small values of the modulation depth ($X < 0.006$) connected with VC structure breaking due to the appearance of the scattering of electrons input velocities that leads to the decrease of the bunched beam current.

To verify results of the simplest theoretical analysis we also consider the possibility of the increasing of output power of the system with a VC within the framework of a self-consistent 1D numerical PIC-model of a low-voltage vircator [30]. The electron beam is simulated by a set of large particles injected into the drift space at regular time intervals. Nonrelativistic equations of motion are solved for each particle and the configuration of the field and the potential of a space charge are determined by solving Poisson equation (for the detailed description of the numerical model see [4,23,7]). The HES input and output of microwaves are simulated with the help of an equivalent circuit approach [31,32].

4. Numerical analysis and discussion of physical processes in the non-autonomous system

The numerical 1D simulation of dynamics of the electron beam in the low-voltage vircator confirms analytically obtained results. Fig. 4 shows the calculated dependencies of output power of a microwave signal on the velocity modulation depth, X, and the frequency of the external harmonic signal, f/f_{VC}. Fig. 4(a) shows that numerically obtained output power demonstrates the behavior being similar to predicted by the analytical model, i.e. output power rises as the depth of the beam modulation X grows. It is a consequence of the preliminary modulation of the electron beam leading to a better formation of electron bunches at the VC region. Unlike the results of the analytical consideration the value X exceeding a certain threshold lowers the level of output microwave power. The further growth of the modulation depth leads to the destruction of the electron bunch in the VC area and increases a current transmitted to the collector. As a consequence, we observe the decrease of output power. The analytical model does not describe this nonlinear effect of the bunch breakdown since we have neglected a transmitted beam current in the theoretical analysis.

Fig. 4(b) demonstrates that the dependence of output power on the external signal frequency, f_m/f_{VC}, has a resonant character. The peak power is observed when the external signal frequency equals to the natural VC oscillations frequency f_{VC}. We can conclude that the velocity modulation of the electron beam leads to the output power growth owing to the development of the most effective electron beam bunching process in the interaction space taking place under certain conditions. Note, that the dependence of output vircator power on the external signal frequency has been studied for different VC oscillation regimes defined by a retarding field in the interaction space ΔV. It is easy to see in Fig. 4(b) that the maximum value of output power is observed for $f_m/f_{VC} = 1.0$ that does not depend on a VC oscillation regime (periodic/wideband generation regime). Let us note that in the case of wideband autonomous generation regime we have observed the transition from wideband oscillations to the periodic-like ones with the growth of

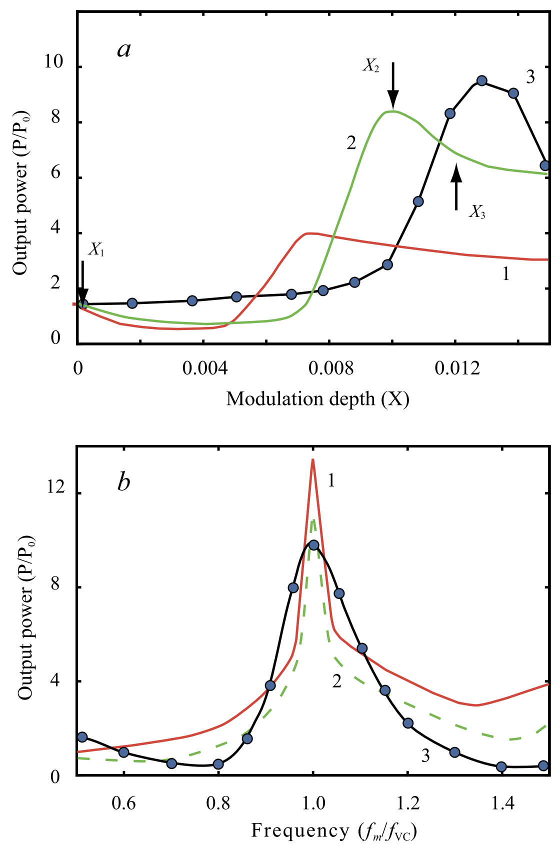

Fig. 4. Results of the numerical simulation (solid lines *1*, *2*) and experimental research (dotted line *3*). The numerically calculated vircator microwave output power versus (a) electron beam velocity pre-modulation depth X and (b) external signal frequency f_m/f_{VC} for different retarding potentials: 1 – $\Delta V = 0.46$ (close to periodic oscillations), 2 – $\Delta V = 0.47$ (wideband oscillations), 3 – $\Delta V = 600$ V (periodic oscillations). In (a) curve *1* is obtained with the dimensionless external force frequency $f_m = 1.24$, curve *2* – $f_m = 1.30$, curve *3* – $f_m = 2.41$ GHz. In (b) curves are plotted for values of X for which output power reaches a maximum value. Arrows denote typical values of the velocity modulation depth.

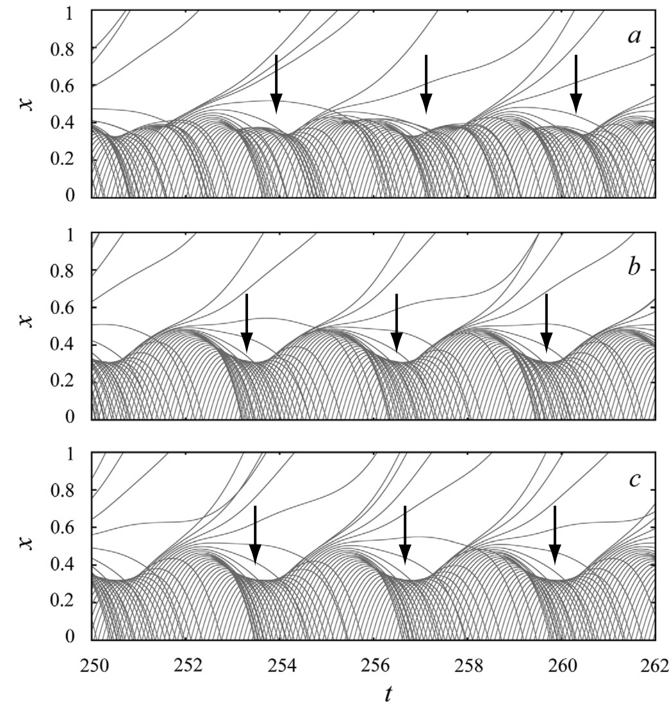

Fig. 5. Space–time diagrams of charged particles dynamics in the drift space of the non-autonomous low-voltage vircator for retarding potential $\Delta V = 0.47$. Three situations are presented: (a) trajectories of electrons in the autonomous vircator ($X_1 = 0.0$, see arrow X_1 in Fig. 4); (b) trajectories of electrons for the optimal magnitude of the velocity pre-modulation depth corresponding to peak output power ($X_2 = 0.0095$, see arrow X_2 in Fig. 4); (c) trajectories of electrons when the velocity pre-modulation depth is greater than the optimal magnitude ($X_3 = 0.0115$, see arrow X_3 in Fig. 4). Arrows point at the areas with the maximal space-charge density (VC formation area).

the external signal amplitude leading to the increase of electron beam pre-modulation depth.

To explore physical processes occurring in the non-relativistic electron beam and leading to the growth of output vircator power we have carried out the analysis of charged particles trajectories in the drift space of the low-voltage vircator. We have considered the case of autonomous regime of wideband VC oscillations where the discovered features of the electron beam dynamics are manifested particularly clearly, but the similar dynamics is observed in the case of external signal influence on the close to periodic autonomous VC oscillations. Fig. 5 shows space–time diagrams of the electron beam in the diode gap for three different typical values of the electron beam pre-modulation depth X_1, X_2 and X_3 (marked by arrows in Fig. 4) corresponding to the autonomous regime, peak power and power decrease. Fig. 5(a) illustrates trajectories of charged particles in the autonomous vircator ($X_1 = 0$). In this case the electron beam is characterized by complex trajectories of charged particles and the complex non-regular dynamics of the VC that reflects electrons periodically. In the space–time diagram the VC (the bunch of electrons) corresponds to regions of the concentration of particles trajectories. As a consequence, the electron bunch (VC) demonstrating chaotic spatial–temporal dynamics is poorly formed.

Fig. 5(b) illustrates the case when there is an external harmonic force modulating the electron beam in the low-voltage vircator. The selected value $X_2 = 0.0095$ corresponds to the peak of output microwave power of the vircator. The pre-modulation of the electron beam makes it possible to keep a stable electron bunch possessing a high space-charge density in the VC area (see Fig. 5(b)). It is important to note that the transmitted current (the current registered on the collector) is close to a minimal value (see Fig. 6 that shows a transmitted current versus a beam modulation depth). This point indicates that the energy of injected particles is not enough to overcome the potential barrier of the VC and the most of them are accumulated in the VC region. So, the dense electron bunch is formed due to the specific space–time dynamics of the pre-modulated electron beam. According to the space-charge density increase the system demonstrates the growth of output microwave radiation amplitude and, as a consequence, the peak of output microwave power.

The further increase of the velocity pre-modulation leads to the decrease of output microwave power. Fig. 5(c) obtained for $X_3 = 0.0115$ gives an explanation of this fact. This effect is connected with the destruction of the VC structure under the influence of the deeper velocity pre-modulation. Fig. 5(c) demonstrates that due to the large electron velocity spread there is a number of charged particles being able to get over the VC potential barrier and, therefore, the transmitted current starts increasing (see Fig. 6 for large values of X). It reduces the current density in the VC area and breaks the dense electron bunch (VC). The decrease of the bunched current in the interaction space of the low-voltage vircator leads to the decrease of output microwave power for large values of the velocity modulation depth.

5. Experimental confirmation of the theoretical and numerical results

The experimental investigation of the non-autonomous low-voltage vircator prototype also confirms results of both the the-

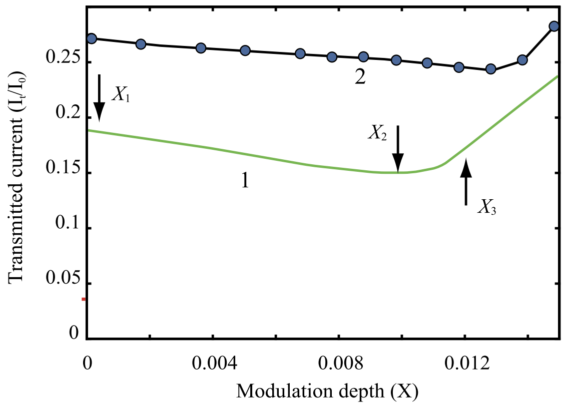

Fig. 6. Dependencies of the normalized current transmitted to the collector of the low-voltage vircator on the velocity pre-modulation depth. Curve *1* corresponds to the numerical simulation (cf. with curve 2 in Fig. 4(a)) and curve *2* — to the experimental study (cf. with curve 3 in Fig. 4(a)).

oretical research and the numerical simulation. As shown in Fig. 4 (curve *3*) the external harmonic signal leads to the output power amplification in the same way as the theoretical analysis predicted. This output power dependence corresponds to the external signal effect on the periodic microwave generation regime in the vircator (see Fig. 2(b)). Power of output microwave radiation grows with increasing the external signal amplitude and has a peak magnitude when the frequency of the external signal is equal to the frequency of a VC electric field oscillations in the autonomous regime. The power of the external microwave signal corresponding to the optimal pre-modulation providing maximal gain in the vircator output power is equal to $P_{ext} = 0.16$ W ($P_{ext}/P_0 = 0.06$) at frequency $f_m = 2.41$ GHz. Such external signal leads to a modulation depth $X \sim 0.0128$. The dynamics of a transmitted current in the experimental vircator model with increasing modulation depth is also in the good agreement with results of the numerical analysis (see Fig. 6, curve *2*). Let us note that we have observed the similar results of the external periodic signal effect on the vircator in the regime of broadband oscillations that is observed in the system at $\Delta V = 860$ V. In this case we have experimentally discovered the growth of the output power about 4 times as compared to the autonomous generation power. At the same time we have also observed the simplifying of the wideband generation spectrum and the transition to the periodic-like oscillations with the increase of external signal power.

6. Conclusion

Obtained results of both theoretical and experimental investigations of the external single-frequency signal effect on the low-voltage vircator show the possibility of the significant power amplification of output microwave power for certain parameters of the external force. The numerical analysis of the dynamics of the electron beam in the interaction space of the vircator system and its experimental verification explains mechanisms of the output power gain in terms of the additional bunching of charged particles and, as a consequence, formation of a denser electron bunch in the VC area owing to the pre-modulation of the electron beam by the external signal with an appropriate frequency and power.

Acknowledgements

This work has been supported by Russian Foundation for Basic Research (Grants 12-02-33071, 12-02-00345, 14-02-31204), President Program (Projects MD-345.2013.2, MK-818.2013.2 and MK-1373.2014.2), and the Ministry of Education and Sciences of Russian Federation.

References

[1] D.J. Sullivan, J.E. Walsh, E.A. Coutsias, Virtual cathode oscillator (vircator) theory, in: V.L. Granatstein, I. Alexeff (Eds.), High Power Microwave Sources, in: Artech House Microwave Library, vol. 13, Artech House, 1987.
[2] V.D. Alyokhin, A.E. Dubinov, V.D. Selemir, O.A. Shamro, N.V. Stepanov, V.E. Vatrunin, Theoretical and experimental studies of virtual cathode microwave devices, IEEE Trans. Plasma Sci. 22 (5) (1994) 945–959.
[3] A.E. Dubinov, V.D. Selemir, Electronic devices with virtual cathodes (review), J. Commun. Technol. Electron. 47 (6) (2002) 575.
[4] Yu.A. Kalinin, A.A. Koronovskii, A.E. Hramov, E.N. Egorov, R.A. Filatov, Experimental and theoretical investigations of stochastic oscillatory phenomena in a nonrelativistic electron beam with a virtual cathode, Plasma Phys. Rep. 31 (11) (2005) 938–952.
[5] J. Benford, J.A. Swegle, E. Schamiloglu, High Power Microwaves, CRC Press, Taylor and Francis, 2007.
[6] D. Biswas, A one-dimensional basic oscillator model of the vircator, Phys. Plasmas 16 (6) (2009) 063104, http://dx.doi.org/10.1063/1.3155472.
[7] R.A. Filatov, A.E. Hramov, Y.P. Bliokh, A.A. Koronovskii, J. Felsteiner, Influence of background gas ionization on oscillations in a virtual cathode with a retarding potential, Phys. Plasmas 16 (3) (2009) 033106.
[8] A.Y. Ender, V.I. Kuznetsov, H. Schamel, Relativistic bursian diode equilibria, Phys. Plasmas 18 (3) (2011) 033502, http://dx.doi.org/10.1063/1.3562115.
[9] G. Singh, C. Shashank, Particle-in-cell simulations for virtual cathode oscillator including foil ablation effects, Phys. Plasmas 18 (2011) 063104.
[10] A.E. Hramov, S.A. Kurkin, A.A. Koronovskii, A.E. Filatova, Effect of self-magnetic fields on the nonlinear dynamics of relativistic electron beam with virtual cathode, Phys. Plasmas 19 (11) (2012) 112101, http://dx.doi.org/10.1063/1.4765062.
[11] S.A. Kurkin, A.E. Hramov, A.A. Koronovskii, Microwave radiation power of relativistic electron beam with virtual cathode in the external magnetic field, Appl. Phys. Lett. 103 (2013) 043507.
[12] R.A. Mahaffey, P.A. Sprangle, J. Golden, C.A. Kapetanakos, High-power microwaves from a non-isochronous reflecting electron system, Phys. Rev. Lett. 39 (13) (1977) 843.
[13] A.S. Shlapakovski, T. Queller, Y. Bliokh, Y.E. Krasik, Investigations of a double-gap vircator at sub-microsecond pulse durations, IEEE Trans. Plasma Sci. 40 (6) (2012) 1607–1617.
[14] S.C. Burkhart, R.D. Scarpetty, R.L. Lundberg, A virtual cathode reflex triode for high power microwave generation, J. Appl. Phys. 58 (1) (1985) 28.
[15] R.F. Hoeberling, M.V. Fazio, Advances in virtual cathode microwave sources, IEEE Trans. Electromagn. Compat. 34 (3) (1992) 252–258.
[16] A.E. Hramov, I.S. Rempen, Investigation of the complex dynamics and regime control in Pierce diode with the delay feedback, Int. J. Electron. 91 (1) (2004) 1–12.
[17] H. Sze, J. Benford, B. Harteneck, Dynamics of virtual cathode oscillator driven by a pinched diode, Phys. Fluids 29 (11) (1986) 3873.
[18] N.N. Gadetskii, I.I. Magda, S.I. Naisteter, Y. Prokopenko, V.I. Tchumakov, The virtode: a generator using supercritical reb current with controlled feedback, Plasma Phys. Rep. 19 (1993) 273.
[19] A.E. Hramov, A.A. Koronovsky, S.A. Kurkin, I.S. Rempen, Chaotic oscillations in electron beam with virtual cathode in external magnetic field, Int. J. Electron. 98 (11) (2011) 1549–1564.
[20] S.A. Kurkin, A.E. Hramov, Virtual cathode formation in annular electron beam in an external magnetic field, Tech. Phys. Lett. 35 (1) (2009) 23–25.
[21] S. Gursharn, C. Shashank, Secondary virtual-cathode formation in a low-voltage vircator: pic simulations, IEEE Trans. Plasma Sci. 36 (3) (2008) 694–700.
[22] A.E. Hramov, A.A. Koronovskii, S. Kurkin, Numerical study of chaotic oscillations in the electron beam with virtual cathode in the external non-uniform magnetic fields, Phys. Lett. A 374 (30) (2010) 3057–3066, http://dx.doi.org/10.1016/j.physleta.2010.05.047.
[23] E.N. Egorov, Y. Kalinin, A.A. Koronovskii, Y. Levin, A.E. Hramov, Analysis of the formation of structures and chaotic dynamics in a nonrelativistic electron beam with a virtual cathode in the presence of a decelerating field, J. Commun. Technol. Electron. 52 (1) (2007) 45.
[24] E.N. Egorov, Y. Kalinin, A.A. Koronovskii, A.E. Hramov, Analysis of the dependence of the microwave generation power of a low-voltage vircator on controlling parameters, Tech. Phys. 52 (10) (2007) 1387.
[25] H. Sze, D. Price, B. Harteneck, Phase locking of two strongly coupled vircators, J. Appl. Phys. 67 (5) (1990) 2278–2282.
[26] K.J. Hendricks, R. Adler, R.C. Noggle, Experimental results of phase locking two virtual cathode oscillators, J. Appl. Phys. 68 (2) (1990) 820–828.
[27] A.E. Dubinov, V.D. Selemir, Vircator generation spectrum controlled by an external SHF signal, Tech. Phys. Lett. 26 (7) (2000) 547–549.
[28] Y. Kalinin, I.S. Rempen, A.E. Hramov, Effect of external signal on oscillations in electron beam with virtual cathode (experiment and numerical analysis), Bull. Russ. Acad. Sci., Phys. 69 (12) (2005) 1936–1941.

[29] M.V. Fazio, J. Kinross-Wright, B. Haynes, R.F. Hoeberling, The virtual cathode microwave amplifier experiment, J. Appl. Phys. 66 (6) (1989) 2675–2677, http://dx.doi.org/10.1063/1.344236.
[30] C.K. Birdsall, A.B. Langdon, Plasma Physics via Computer Simulation, Taylor and Francis Group, 2005.
[31] E.N. Egorov, Y. Kalinin, A.A. Koronovskii, A.E. Hramov, M. Morozov, Microwave generation power in a nonrelativistic electron beam with virtual cathode in a retarding electric field, Tech. Phys. Lett. 32 (5) (2006) 402–405.
[32] I.J. Morey, C.K. Birdsall, Travelling-wave-tube simulation: the IBC code, IEEE Trans. Plasma Sci. 18 (3) (1990) 482.